Enhancement of Superconductivity near the Ferromagnetic Quantum Critical Point in UCoGe

E. Slooten,[1] T. Naka,[2] A. Gasparini,[1] Y. K. Huang,[1] and A. de Visser[1,*]

[1]*Van der Waals-Zeeman Institute, University of Amsterdam, Valckenierstraat 65, 1018 XE Amsterdam, The Netherlands*
[2]*National Research Institute for Materials Science, Sengen 1-2-1, Tsukuba, Ibaraki 305-0047, Japan*

We report a high-pressure single crystal study of the superconducting ferromagnet UCoGe. Measurements of the ac susceptibility and resistivity under pressures up to 2.2 GPa show ferromagnetism is smoothly depressed and vanishes at a critical pressure $p_c = 1.4$ GPa. Near the ferromagnetic critical point superconductivity is enhanced. Upper-critical field measurements under pressure show $B_{c2}(0)$ attains remarkably large values, which provides solid evidence for spin-triplet superconductivity over the whole pressure range. The obtained p-T phase diagram reveals superconductivity is closely connected to a ferromagnetic quantum-critical point hidden under the superconducting "dome."

The recent discovery of superconductivity in itinerant-electron ferromagnets tuned to the border of ferromagnetic order [1–4] disclosed a new research theme in the field of magnetism and superconductivity. Notably, superconducting ferromagnets provide a unique testing ground [1,5] for superconductivity not mediated by phonons, but by magnetic interactions associated with a magnetic quantum-critical point (QCP) [6–8]. In the "traditional" model for spin-fluctuation mediated superconductivity [6] a second-order ferromagnetic quantum phase transition takes place when the Stoner parameter diverges, and near the critical point the exchange of longitudinal spin fluctuations stimulates spin-triplet superconductivity. Superconductivity is predicted to occur in the ferromagnetic as well as in the paramagnetic phase, while at the critical point the superconducting transition temperature $T_s \rightarrow 0$. Research into ferromagnetic superconductors will help to unravel how magnetic fluctuations can stimulate superconductivity. This novel insight might turn out to be crucial in the design of new superconducting materials.

High-pressure experiments have been instrumental in investigating the interplay of magnetism and superconductivity. In the case of UGe$_2$ [1] superconductivity is found only in the ferromagnetic phase under pressure close to the critical point, and at the critical pressure, p_c, ferromagnetism and superconductivity disappear simultaneously. The ferromagnetic transition becomes first order for $p \rightarrow p_c = 1.6$ GPa [9]. Moreover, a field-induced first-order transition between two states with different polarizations was found in the ferromagnetic phase [10]. Superconductivity is attributed to critical magnetic fluctuations associated with this first-order metamagnetic transition [11], rather than with critical spin fluctuations near p_c. In UIr the ferro-to-paramagnetic phase transition remains second order under pressure all the way to $p_c = 2.8$ GPa [3,12]. Superconductivity appears in the ferromagnetic phase in a small pressure range close to p_c, however, it is not observed for $p \gtrsim p_c$, which is at variance with the traditional spin-fluctuation model [6]. In URhGe [2] ferromag-

netism and superconductivity are observed at ambient pressure. Pressure raises the Curie temperature, T_C, and drives the system away from the magnetic instability [13]. Compelling evidence has been presented that p-wave superconductivity in URhGe is mediated by critical magnetic fluctuations associated with a field-induced spin-reorientation process [5]. Moreover, the same spin-reorientation process gives rise to a remarkable reentrant superconducting phase near the high-field first-order quantum-critical end point [14].

In this Letter we show that the response to pressure of the superconducting ferromagnet UCoGe is manifestly different. While ferromagnetism is gradually depressed and vanishes near $p_c = 1.4$ GPa, superconductivity is enhanced and survives in the paramagnetic phase at least up to 2.2 GPa. The superconducting state is remarkably robust under influence of a magnetic field, which provides solid evidence for spin-triplet superconductivity at both sides of p_c. The p-T phase diagram reveals superconductivity is closely connected to a ferromagnetic QCP hidden under the superconducting "dome."

UCoGe crystallizes in the orthorhombic TiNiSi structure (space group P_{nma}) [15]. At zero pressure UCoGe undergoes a ferromagnetic transition at the Curie temperature $T_C = 3$ K [4]. Magnetization measurements on a single crystal [16] show that the ordered moment is small, $m_0 = 0.07\mu_B$, and directed along the orthorhombic c axis. UCoGe is a weak itinerant ferromagnet as follows from the small ratio of m_0 compared to the Curie-Weiss effective moment ($p_{\text{eff}} = 1.7\mu_B$), and the small value of the magnetic entropy associated with the magnetic phase transition [4]. Muon-spin relaxation measurements [17] provide unambiguous proof that weak magnetism is a bulk property which coexists with superconductivity. For a high-quality single crystal with $RRR = 30$ (RRR is the ratio of the electrical resistance measured at room temperature and 1 K), superconductivity is found with an onset temperature in the resistance $R(T)$ of $T_s^{\text{onset}} = 0.6$ K [16]. Specific-heat and thermal-expansion data [4] were used to calculate the

rates of change of T_C and T_s with pressure with help of the Ehrenfest relation for second-order phase transitions: $T_C/dp = -2.5$ K/GPa and $dT_s/dp = 0.2$ K/GPa. This hinted at a relatively low critical pressure $p_c \sim 1.2$ GPa for the disappearance of ferromagnetic order.

The high-pressure measurements were made using a hybrid clamp cell made of NiCrAl and CuBe alloys. Samples were mounted on a dedicated plug which was placed in a Teflon cylinder with Daphne oil 7373 as a hydrostatic pressure transmitting medium. The pressure cell was attached to the cold plate of a ^{3}He refrigerator with a base temperature $T = 0.24$ K. The pressure was monitored by the superconducting transition temperature of lead. The ac susceptibility (with frequency range $f = 113$–313 Hz and driving field $B_{ac} \sim 10^{-6}$ T) and ac resistivity ($f = 13$ Hz) were measured using lock-in techniques with a low excitation current ($I = 100$–300 μA). The single crystals studied were previously used in Ref. [16]. The ac susceptibility was measured on a bar-shaped sample with $B_{ac} \parallel c$ axis (long direction of the bar). For the resistivity measurements 2 bar-shaped samples with the current I along the a axis and c axis were mounted in the pressure cell. The suppression of superconductivity by a magnetic field was investigated by resistivity measurements in fixed magnetic fields $B\|I\|a$ and $B\|I\|c$.

In Fig. 1 we show the temperature variation of the ac susceptibility $\chi_{ac}(T)$ around the magnetic and superconducting transitions at applied pressures up to 2.18 GPa. The Curie temperature, signaled by the maximum in $\chi_{ac}(T)$, steadily decreases with increasing pressure up to 1.03 GPa.

For $p \gtrsim 1.11$ GPa the (complete) magnetic transition is no longer observed. The bulk superconducting transition temperature, T_s^χ, is identified by the midpoint of the transition to the diamagnetic state. The width of the superconducting transition $\Delta T_s^\chi \simeq 0.10$ K and does not change as a function of pressure. T_s^χ increases for pressures up to $p = 1.11$ GPa, where it attains a maximum value of 0.60 K. For larger pressures T_s^χ decreases as shown in the inset of Fig. 1. The magnitude of the diamagnetic signal amounts to 80% of the ideal screening value [4] and does not vary as a function of pressure, which confirms superconductivity is a bulk property up to the highest pressure.

By taking the values of T_C and T_s^χ from the $\chi_{ac}(T)$ data, we construct the pressure-temperature phase diagram shown in Fig. 2. In the diagram we have also plotted the magnetic and superconducting transition temperatures extracted from resistivity data, $\rho(T)$, taken in a separate high-pressure run. Here T_C is identified by a kink in $\rho(T)$ [16] and the superconducting transition temperature, T_s^R, is taken as the midpoint to the zero resistance state. The width of the superconducting transition $\Delta T_s^R \leq 0.10$ K at all pressures. The values of T_s^R systematically exceed T_s^χ, in agreement with the earlier observation [4] that the diamagnetic signal appears when the resistive transition is complete. For $p \gtrsim 0.4$ GPa T_C follows a linear suppression at a rate of -2.4 K/GPa. The phase line $T_C(p)$ intersects the superconducting phase boundary near $p \approx 1.16$ GPa, and its linear extrapolation yields the critical
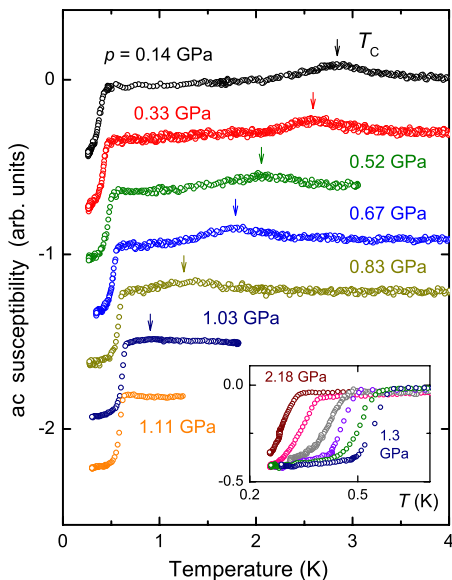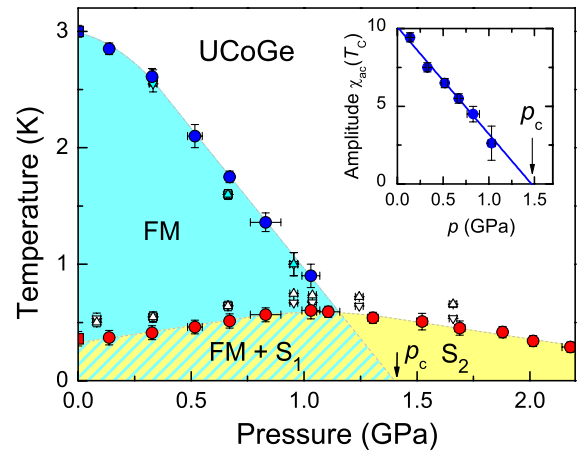

FIG. 1 (color online). The ac susceptibility of UCoGe plotted versus temperature at different pressures as indicated. The curves are offset along the vertical axis for clarity. The arrows indicate T_C. The inset shows $\chi_{ac}(T)$ around the superconducting transition measured at pressures (from right to left) of 1.30, 1.52, 1.69, 1.88, 2.01, and 2.18 GPa.

FIG. 2 (color online). Pressure-temperature phase diagram of UCoGe. Ferromagnetism (FM), blue area; superconductivity (S_1, S_2), yellow area. $T_C(p)$ extrapolates to a ferromagnetic QCP at the critical pressure $p_c = 1.40 \pm 0.05$ GPa. Superconductivity coexists with ferromagnetism below p_c, blue-yellow hatched area. Symbols: filled blue and red circles T_C and T_s^χ from $\chi_{ac}(T)$; blue and white triangles T_C and T_s^R from $\rho(T)$ (up triangles $I \parallel a$ axis, down triangles $I \parallel c$ axis); filled blue and red squares T_C and T_s^χ at $p = 0$ taken from a polycrystal [4]. Inset: Amplitude of $\chi_{ac}(T)$ at T_C as a function of pressure. The data follow a linear p dependence and extrapolate to $p_c = 1.46 \pm 0.10$ GPa.

pressure for the suppression of ferromagnetic order $p_c = 1.40 \pm 0.05$ GPa. An almost equal value $p_c = 1.46 \pm 0.10$ GPa is deduced from the pressure variation of the amplitude of χ_{ac} at T_C (inset Fig. 2). The data reveal the magnetic transition is continuous over the entire pressure range—hysteresis in the magnetic signal is absent—and consequently ferromagnetic order vanishes at a second-order quantum-critical point. As we cannot detect the weak χ_{ac} signal at T_C in the superconducting phase, the possibility that T_C vanishes abruptly near $p = 1.1$ GPa cannot be ruled out completely. In this case the nature of the phase transition becomes first order, and the phase line $T_C(p)$ terminates at a first-order quantum end point [18].

The high-pressure data irrevocably demonstrate that superconductivity persists in the paramagnetic regime. This marks a pronounced difference with the other superconducting ferromagnets, in which superconductivity is confined to the ferromagnetic state. The phase diagram shown in Fig. 2 clarifies a comparable diagram obtained by a high-pressure transport study on a polycrystalline sample [19] with relatively broad magnetic and superconducting transitions, which hampered notably a proper determination of $T_C(p)$. We identify the characteristic pressure $p^* \approx 0.8$ GPa at which a change in the superconducting properties was reported [19] as the pressure $p \approx 1.16$ GPa at which T_C drops below T_s.

The presence of a second-order ferromagnetic QCP under the superconducting dome may provide an essential clue for understanding superconductivity in UCoGe. The phase diagram of UCoGe, reported in Fig. 2, does not obey the traditional spin-fluctuation scenario [6], as T_s remains finite at p_c. Clearly, more sophisticated models [20–22] are needed. Notice, a nonzero transition temperature at p_c was obtained in Ref. [20], where the spin-triplet pairing strength in the paramagnetic regime was investigated using an Eliashberg treatment and imposing a strong Ising anisotropy of the critical fluctuations.

UCoGe is unique because it is the only superconducting ferromagnet which has a superconducting phase in the paramagnetic regime. Symmetry-group considerations [23] tell us that this state (which we label S_2) differs from the superconducting state (label S_1) in the ferromagnetic phase. In the paramagnetic state ($T > T_C > T_s$) the symmetry group is given by $G^{\text{sym}} = G \times T \times U(1)$, where G represents the point-group symmetry of the orthorhombic lattice, T denotes time-reversal symmetry, and $U(1)$ is gauge symmetry. Below T_C time-reversal symmetry is broken, and in the superconducting phase S_1 gauge symmetry is broken as well. However, in the paramagnetic superconducting regime the phase S_2 breaks only gauge symmetry. For uniaxial ferromagnets with orthorhombic crystal symmetry, the possible unconventional superconducting states in the presence of strong spin-orbit coupling have been worked out in detail [23], and can be discriminated in close analogy with the familiar superfluid phases

of ^{3}He [24]. In the ferromagnetic phase, exchange splitting results in spin-up and spin-down Fermi surfaces. At both Fermi surfaces an attractive pairing potential may give rise to Cooper pairs, which form from electrons with opposite momentum and necessarily have the same spin. Consequently, a superconducting ferromagnet is essentially a nonunitary two-band superconductor [23,24] with equal-spin pairing Cooper states $|\uparrow\uparrow\rangle$ and $|\downarrow\downarrow\rangle$. Below T_C, the superconducting phase is similar to the A_2 phase of liquid ^{3}He (i.e., the A phase in field), which is a linear combination of the Cooper pair states $|S_z = 1, m = 1\rangle$ and $|S_z = -1, m = 1\rangle$ with different populations [24]. In the paramagnetic state the degeneracy of the spin-up and spin-down band is restored, as well as time-reversal symmetry. There are two candidate states [24] for S_2: (i) a conventional spin-singlet state or (ii) a unitary spin-triplet state, like the planar state of superfluid ^{3}He, which is an equally weighted superposition of the two states with $|S_z = 1, m = -1\rangle$ and $|S_z = -1, m = 1\rangle$. In the following paragraph we present measurements of the upper-critical field B_{c2} under pressure, which provide evidence for the latter scenario.

The suppression of superconductivity by a magnetic field was investigated at selected pressures by electrical resistivity measurements in fixed magnetic fields. The results are reported in Fig. 3. The upper-critical field for $B \parallel a$, B_{c2}^a, shows a remarkable enhancement on approach of the critical pressure p_c. By comparing with the tem-
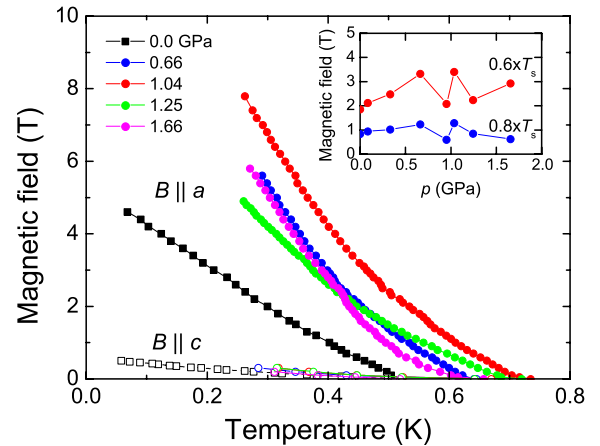

FIG. 3 (color online). Temperature variation of the upper-critical field of UCoGe at different pressures. Data points are collected from resistance data, measured in fixed fields $B \parallel a$ (filled symbols) and $B \parallel c$ (open symbols). The error bars are given by the size of the symbols. $T_s^R(B)$ is taken at the midpoint of the transition to $R = 0$. Data for this sample at $p = 0$ are taken from Ref. [16]. For $B \parallel a$, B_{c2} shows a strong enhancement on approach of the critical pressure p_c (blue, red and green curves). B_{c2} remains large at 1.66 GPa in the paramagnetic phase (magenta curve). For $B \parallel c$ the data taken at various pressures almost overlap. Inset: $B_{c2}(p)$ at $0.6T_s$ and $0.8T_s$ after normalization $T_s(p)/T_s(p = 0) = 1$ for $B = 0$. The error bars are given by the size of the symbols.

perature variation $B_{c2}^a(T)$ at ambient pressure [16], we arrive at a conservative estimate for $B_{c2}^a(T \rightarrow 0)$ of 15 T near p_c, which exceeds the ambient pressure value by a factor 3. B_{c2}^a remains large in the whole pressure range as demonstrated in the inset of Fig. 3, where the critical field at $0.6T_s$ and $0.8T_s$ (where T_s is the reduced temperature) is plotted versus pressure. The large values of $B_{c2}^a(T \rightarrow 0)$ provide solid evidence for spin-triplet Cooper pairing, as the Pauli paramagnetic limit for spin-singlet superconductivity $B_{c2}^{\text{Pauli}} \approx 1.83T_s = 1.3$ T. Thus the data taken in the paramagnetic phase at $p = 1.66$ GPa lead to the important conclusion that spin-triplet superconductivity, most likely with a ^{3}He-like planar-state [24], persists in the paramagnetic phase. The anisotropy $B_{c2}^a \gg B_{c2}^c$ yields support [16] for an axial superconducting gap function with point nodes along the direction (c axis) of the ordered moment m_0. This anisotropy is preserved under pressure.

Finally, we turn to the unusual upward curvature in $B_{c2}^a(T)$. For three-dimensional materials an upward curvature in $B_{c2}(T)$ is normally a signature of two-band (or multiple-band) superconductivity [25]. For a two-band ferromagnetic superconductor it can naturally be attributed [16,23] to the field-induced population redistribution of the states $|\uparrow\uparrow\rangle$ and $|\downarrow\downarrow\rangle$. This calls for theoretical calculations of B_{c2} using a linearized Ginzburg-Landau equation including gradient terms [23] for the orthorhombic symmetry case. The intricate nonmonotonic variation of T_s with field and pressure is possibly related to a rapid variation of the different anisotropy coefficients of the gradient terms near the critical point. We stress, however, that the observed variation in $B_{c2}(T, p)$ is an intrinsic property and largely exceeds the experimental uncertainty. Another interesting scenario for the upward curvature in B_{c2} is the proximity to a field-induced QCP, like reported [5,14] for URhGe. However, high-field magnetoresistance data taken at ambient pressure [26] have not revealed a metamagnetic transition so far ($B \leq 30$ T).

In conclusion, we have measured the p-T phase diagram of the superconducting ferromagnet UCoGe for high-quality single crystals. Ferromagnetism is smoothly depressed and vanishes at the critical pressure $p_c = 1.4$ GPa. Near the ferromagnetic critical point, T_s goes through a maximum and superconductivity is enhanced. The upper-critical field $B_{c2}(T)$ shows an unusual upward curvature, which extrapolates to remarkably large values of $B_{c2}(0)$ at both sides of p_c. This provides solid evidence for spin-triplet superconductivity over the whole pressure range. The obtained p-T phase diagram is manifestly different from that of other superconducting ferromagnets, notably because superconductivity is enhanced near p_c and persists in the paramagnetic phase. This reveals supercon-

ductivity is closely connected to a ferromagnetic QCP hidden under the superconducting dome. We conclude the p-T-B phase diagram of UCoGe provides a unique opportunity to explore unconventional superconductivity stimulated by magnetic interactions.

*a.devisser@uva.nl

[1] S. S. Saxena et al., Nature (London) **406**, 587 (2000).
[2] D. Aoki et al., Nature (London) **413**, 613 (2001).
[3] T. Akazawa et al., J. Phys. Condens. Matter **16**, L29 (2004).
[4] N. T. Huy et al., Phys. Rev. Lett. **99**, 067006 (2007).
[5] F. Lévy et al., Science **309**, 1343 (2005).
[6] D. Fay and J. Appel, Phys. Rev. B **22**, 3173 (1980).
[7] G. G. Lonzarich, in Electron: A Centenary Volume, edited by M. Springford (Cambridge University Press, Cambridge, England, 1997), Chap. 6.
[8] P. Monthoux, D. Pines, and G. G. Lonzarich, Nature (London) **450**, 1177 (2007).
[9] T. Terashima et al., Phys. Rev. Lett. **87**, 166401 (2001).
[10] C. Pfleiderer and A. D. Huxley, Phys. Rev. Lett. **89**, 147005 (2002).
[11] K. G. Sandeman, G. G. Lonzarich, and A. J. Schofield, Phys. Rev. Lett. **90**, 167005 (2003).
[12] T. C. Kobayashi et al., J. Phys. Soc. Jpn. **76**, 051007 (2007).
[13] F. Hardy et al., Physica (Amsterdam) **359–361B**, 1111 (2005).
[14] F. Lévy, I. Sheikin, and A. Huxley, Nature Phys. **3**, 460 (2007).
[15] F. Canepa et al., J. Alloys Compd. **234**, 225 (1996).
[16] N. T. Huy et al., Phys. Rev. Lett. **100**, 077002 (2008).
[17] A. de Visser et al., Phys. Rev. Lett. **102**, 167003 (2009).
[18] D. Belitz, T. R. Kirkpatrick, and T. Vojta, Phys. Rev. Lett. **82**, 4707 (1999).
[19] E. Hassinger et al., J. Phys. Soc. Jpn. **77**, 073703 (2008).
[20] R. Roussev and A. J. Millis, Phys. Rev. B **63**, 140504(R) (2001).
[21] P. Monthoux and G. G. Lonzarich, Phys. Rev. B **63**, 054529 (2001).
[22] D. Belitz and T. R. Kirkpatrick, Phys. Rev. B **69**, 184502 (2004).
[23] V. P. Mineev and T. Champel, Phys. Rev. B **69**, 144521 (2004).
[24] V. P. Mineev, arXiv:0812.2171v1.
[25] S. V. Shulga et al., Phys. Rev. Lett. **80**, 1730 (1998).
[26] A. Gasparini, J. Giesbers, U. Zeitler, and A. de Visser (unpublished).